MJFAS
Malaysian Journal of Fundamental and Applied Sciences

Munir *et al.* | Malaysian Journal of Fundamental and Applied Sciences, Vol. 18 (2022) 430-447

RESEARCH ARTICLE

Analysis of Unsteady Solute Dispersion in a Blood Flow of Herschel-Bulkley through a Catheterized Stenosed Artery

Intan Diyana Munir, Nurul Aini Jaafar*, Sharidan Shafie

Department of Mathematical Sciences, Faculty of Science, Universiti Teknologi Malaysia, 81310 UTM Johor Bahru, Johor, Malaysia

Abstract Blockage of blood flow due to cholesterol deposits at the arterial wall, known as stenosis, can lead to conditions such as heart attack and stroke. Treatment such as balloon angioplasty involves the catheterization of an artery where a stented catheter is inflated at the stenosis site to open the narrowed artery. The catheterization of the stenosed artery affects the surrounding blood flow and dispersion process. The present study analyses the effect of catheter radius and stenosis height on the blood velocity and solute dispersion behavior. Herschel-Bulkley fluid is used to model the problem with stenosis as the boundary condition. The momentum equation and Herschel-Bulkley constitutive equation are solved analytically into integral forms. Simpson's 3/8 rule and Regula-Falsi method were used to evaluate the integral numerically to obtain the velocity. The velocity was utilized to solve the unsteady convective-diffusion equation using the generalized dispersion model (GDM) to obtain the dispersion function. This present research can potentially help the medical field and industry in determining the suitable catheter radius for patients, calculating drug dosage and improving stent catheter design. Results show that the velocity decreases as the catheter radius and stenosis height increase. A decrease in velocity simultaneously increases the solute dispersion function.

Keywords: Steady flow, Unsteady solute dispersion, Catheterized artery, Herschel-Buckley model, Stenosis.

Introduction

Atherosclerosis is a cardiovascular disease caused by the build-up of plaque on the wall of the artery. The build-up of plaque eventually causes the interior space of the artery, known as the lumen, to further narrow and interfere with the blood flowing through the artery. The narrowing of the artery caused by plaque build-up is also known as stenosis. Since the function of arteries is to carry blood from the heart to the rest of the body, it is natural for arteries to have a thick wall and small lumen diameter to accommodate the high pressure produced by the pumping action of the heart. Thus, the natural small lumen diameter of the artery, coupled with the presence of stenosis, could potentially lead to fatal heart disease. One of the treatments for stenosis is inserting a catheter through the artery to either diagnose the disease or perform the treatment. Angiography is the technique used to diagnose stenosis in coronary arteries, while angioplasty is the treatment procedure for such artery conditions [1]. When the catheter is inserted into a stenosed artery, the flow dynamics inside the artery changes accordingly. The presence of catheter and stenosis affect both blood flow and solute dispersion behavior inside the artery, further affecting other situations such as the condition of the patient, the treatment effectiveness, the rate of medicine dispersion and many more. Therefore, before carrying out the procedure, doctors should consider the effects of catheters and stenosis to make the treatment more effective and reduce complications. This present study can help give insights into the blood flow and solute dispersion

***For correspondence:**
nurulaini.jaafar@utm.my

Received: 1 October 2021
Accepted: 24 August 2022

behavior inside a catheterized stenosed artery and help improve the medical field in the treatment of atherosclerosis.

In representing blood rheology, the Newtonian and various types of non-Newtonian models have been used by researchers in conducting their study. The simplest non-Newtonian model is the Maxwell model [2]. The selection of the fluid model in representing the blood rheology depends on the type of problem. For example, blood behaves like a non-Newtonian fluid in small arteries at low shear rates [3]. One of the non-Newtonian fluids is the Casson fluid model, which is widely used for blood flow in narrow arteries [4]. For instance, Nagarani et al. [5] analyzed the unsteady dispersion through a catheterized artery using the Casson model. Their study noted that the combined effect of the non-Newtonian rheology of the Casson model and the catheterization of the artery significantly reduced the effective diffusion coefficient. Moreover, Sarojamma et al. [6] conducted a study on the blood flow through a catheterized artery with the presence of stenosis and body acceleration using the Casson model and reported noticeable results of flow pattern and frictional resistance. However, in small arteries branching out to the capillaries known as arterioles which have a diameter of less than 65 μm, the velocity profiles can be explained by the Herschel-Bulkley model but do not conform to the Casson model [7]. Additionally, it is also stated by Chaturani and Ponnalagar Samy [8] that blood behaves like the Herschel-Bulkley model rather than the Power Law and Bingham model in the tube with a diameter of 95 μm. Apart from that, Sankar and Lee [9] adopted the Herschel-Bulkley model in their study on blood flow through a catheterized artery. Moreover, Sankar and Hemalatha [10] studied the blood flow through a catheterized artery using the Herschel-Bulkley model. Meanwhile, Abidin et al. [11] analyzed the flow and solute dispersion through a stenosed artery with the presence of a chemical reaction using the Herschel-Bulkley model. This present study focuses on the blood flow through a narrow artery. Therefore, a fluid model suitable for small artery diameter and low shear rates should be chosen. Since the Herschel-Bulkley model can explain the blood flow behavior through a narrow artery, it is justified to represent the blood rheology using the Herschel-Bulkley model.

To investigate the solute dispersion through the catheterized artery, the generalized dispersion model (GDM) is used to solve the dispersion function. Fundamentally, the concept of axial solute dispersion was first introduced by Taylor [12] by investigating the unsteady solute dispersion in a Newtonian flow through a circular pipe. Moreover, Aris [13] extended the study by considering the axial diffusion term, which was neglected by Taylor [12] using the method of moments. The GDM was later introduced by Gill and Sankarasubramanian [14] for solving the unsteady solute dispersion through a circular pipe to describe the dispersion coefficient with the time parameter. Furthermore, Nagarani et al. [15] studied solute dispersion in the Casson model through an annulus with wall absorption and solved the dispersion coefficient using the GDM. They stated that the presence of a catheter and the non-Newtonian character of the fluid significantly affects the dispersion coefficient. Ramana and Sarojamma [16] investigated solute dispersion in a Herschel-Bulkley model through an annulus using the GDM. Their results showed that the dispersion coefficient decreases as the yield stress and catheter size increase. On the other hand, Nagarani and Sebastian [17] studied the unsteady dispersion in a Casson model flowing through a catheterized artery and used the GDM in solving the dispersion coefficient. They reported that the increase in catheter size decreases the dispersion coefficient. The consistency of the result from the studies mentioned shows that the GDM is a reliable method for obtaining the dispersion coefficient.

Herschel-Bulkley model is suitable to represent the blood rheology in this present study because it can explain the blood flow behavior in a narrow artery with low shear rates. In solving for the dispersion coefficient, the GDM has been adopted. Even though several researchers have utilized the Herschel-Bulkley model in their study, the blood flow behavior represented by a Herschel-Bulkley model in a catheterized stenosed artery has yet to be explored. This present study aims to investigate the influence of catheter radius and stenosis height on the blood flow velocity and solute dispersion function.

Mathematical Formulation

Governing Equations

Consider the dispersion of a solute in blood flowing through a catheterized artery with the presence of

stenosis at the wall of the artery. The blood flow is modelled by the steady, laminar, fully-developed non-Newtonian Herschel-Bulkley model through a catheterized artery with a radius $\bar{R}$. The radius of the catheter is k, where $k < 1$. Figure 1 shows the geometry of the flow through the catheterized artery where $\bar{r}$ is the radius, $\bar{z}$ is the axial direction of the fluid flow, k is the dimensionless catheter radius, λ_1 is the plane location of the lower part of the plug flow region, λ_2 is the plane location of the upper part of the plug flow region, δ is the stenosis height, l_0 is the stenosis length and $\bar{R}(\bar{z})$ is the radius of the stenosed artery. The blood flows through the region between the wall of the artery and the wall of the catheter, which is then further divided into three regions, as shown in Figure 1. The radiuses of these three regions are $k < \bar{r} < \lambda_1$ for the bottom outer flow region, $\lambda_1 < \bar{r} < \lambda_2$ for the plug flow region and $\lambda_2 < \bar{r} < \bar{R}$ for the top outer flow region. The outer flow region is differentiated into the top and bottom regions because the fluid velocities in those two regions are different. Cylindrical polar coordinates are used in the formulation and computation of this present study.

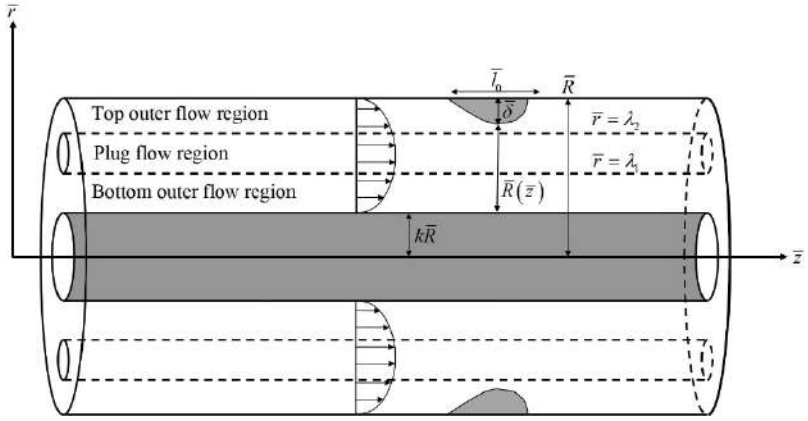

Figure 1. The geometry of blood flow through a catheterized artery.

This present study focuses on the axial flow of the Herschel-Bulkley model. Therefore, the velocity in the radial and azimuthal directions are zero. The axial symmetry leads to the uniformity and independence of the velocity in the $\bar{z}$ direction from the radial and azimuthal directions. Hence, the continuity equation in the $\bar{z}$ direction for the steady flow in a cylindrical coordinate can be simplified to

$$\frac{\partial \bar{w}}{\partial \bar{z}} = 0, \tag{1}$$

where $\bar{w}$ is the fluid velocity in the $\bar{z}$ direction. The momentum equation for steady flow is

$$\frac{d\bar{p}}{d\bar{z}} = -\frac{1}{\bar{r}}\frac{d}{d\bar{r}}(\bar{r}\,\bar{\tau}), \quad k\bar{R} \le \bar{r} \le \bar{R}, \tag{2}$$

where $\bar{p}$ is the pressure and $\bar{\tau}$ is the shear stress. The pressure gradient $d\bar{p}/d\bar{z}$ is considered as a constant. The boundary conditions for the momentum equation in Equation (2) are

$$\begin{aligned} \bar{\tau} &= -\bar{\tau}_y \text{ at } \bar{r} = \lambda_1, \\ \bar{\tau} &= \bar{\tau}_y \text{ at } \bar{r} = \lambda_2, \end{aligned} \tag{3}$$

where $\bar{\tau}_y$ is the yield stress. According to Sankar and Hemalatha [18], the constitutive equation of the Herschel-Bulkley fluid is defined as

$$\begin{aligned} |\bar{\tau}| &= \bar{\mu}_H^{1/n}\left(-\frac{\partial \bar{w}}{\partial \bar{r}}\right)^{1/n} + \bar{\tau}_y \quad \text{if} \quad |\bar{\tau}| \geq \bar{\tau}_y, \\ \frac{\partial \bar{w}}{\partial \bar{r}} &= 0 \quad \text{if} \quad |\bar{\tau}| < \bar{\tau}_y, \end{aligned} \tag{4}$$

where $\bar{\mu}_H$ is the viscosity of Herschel-Bulkley fluid, and n is the power-law index. Equation (4) can now be written as

$$\bar{\mu}_H\left(\frac{\partial \bar{w}}{\partial \bar{r}}\right) = -\left(|\bar{\tau}| - \bar{\tau}_y\right)^n \quad \text{if} \quad |\bar{\tau}| \geq \bar{\tau}_y, \tag{5}$$

with the boundary conditions of

$$\begin{aligned} \bar{w} &= 0 \ \text{ at } \bar{r} = \bar{k}\,\bar{R}, \\ \bar{w} &= 0 \ \text{ at } \bar{r} = \bar{R}(\bar{z}), \end{aligned} \tag{6}$$

where $\bar{R}(\bar{z})$ is the size of stenosis given by Jaafar et al. [19] as

$$\bar{R}(\bar{z}) = \begin{cases} \bar{R} & \text{otherwise}, \\ \bar{R} - \dfrac{\bar{\delta}}{2}\left[1 + \cos\left(\dfrac{2\pi}{\bar{l}_0}\left(\bar{z} - \bar{d} - \dfrac{\bar{l}_0}{2}\right)\right)\right] & \text{when} \quad \bar{d} \leq \bar{z} \leq \bar{l}_0 + \bar{d}. \end{cases} \tag{7}$$

Here, $\bar{\delta}$ is the stenosis height, $\bar{l}_0$ is the stenosis length and $\bar{d}$ is the stenosis location. The simplified unsteady convective-diffusion equation for the dispersion of solute for the Herschel-Bulkley model is given as

$$\frac{\partial \bar{C}}{\partial \bar{t}} + \bar{w}\frac{\partial \bar{C}}{\partial \bar{z}} = \bar{D}_m\left(\frac{1}{\bar{r}}\frac{\partial}{\partial \bar{r}}\left(\bar{r}\frac{\partial}{\partial \bar{r}}\right) + \frac{\partial^2}{\partial \bar{z}^2}\right)\bar{C}, \tag{8}$$

where $\bar{C}$ is the solute concentration, $\bar{t}$ is the time and $\bar{D}_m$ is the molecular diffusivity. The initial and boundary conditions for the convective-diffusion equation in Equation (8) is given by

$$\begin{aligned} \bar{C}(\bar{r}, \bar{z}, 0) &= \bar{C}_0 \quad \text{if} \quad |\bar{z}| \leq \bar{z}_s/2, \\ \bar{C}(\bar{r}, \bar{z}, 0) &= 0 \quad \text{if} \quad |\bar{z}| > \bar{z}_s/2, \end{aligned} \tag{9}$$

$$\bar{C}(\bar{r}, \infty, \bar{t}) = 0, \tag{10}$$

and

$$\frac{\partial \bar{C}}{\partial \bar{r}}(k, \bar{z}, \bar{t}) = \frac{\partial \bar{C}}{\partial \bar{r}}(\bar{R}(\bar{z}), \bar{z}, \bar{t}) = 0, \tag{11}$$

where $\bar{C}_0$ is the reference solute concentration and $\bar{z}_s$ is the solute length.

Method of Solution

Solution for flow velocity

The non-dimensional variables are introduced as follows:

$$w=\frac{\bar{w}}{\bar{w}_0},\quad r=\frac{\bar{r}}{\bar{R}},\quad z=\frac{\bar{z}}{\bar{R}},\quad \tau=\frac{2\bar{\tau}}{\bar{p}_0\bar{R}},\quad C=\frac{\bar{C}}{\bar{C}_0},\quad t=\frac{\bar{D}_m\bar{t}}{\bar{R}^2},\quad R(z)=\frac{\bar{R}(\bar{z})}{\bar{R}},\quad d=\frac{\bar{d}}{\bar{R}},\quad l_0=\frac{\bar{l}_0}{\bar{R}},\quad \delta=\frac{\bar{\delta}}{\bar{R}}, \tag{12}$$

where w, r, z, τ, C, t, R(z), d, l_0 and δ is the non-dimensional variables of velocity, radius, axial coordinate, shear stress, concentration, time, stenosis size, stenosis location, stenosis length and stenosis height, respectively and $\bar{p}_0$ is the absolute magnitude of the typical pressure gradient. The pressure gradient can be written as $d\bar{p}/d\bar{z}=-\bar{p}_0 p_s$, where p_s is the static pressure gradient. The viscosity $\bar{\mu}$ is $\bar{\mu}=\bar{\mu}_H(2/\bar{p}_0\bar{R})^{n-1}$ with the dimension of Newtonian fluid's viscosity. The non-dimensional variables are substituted into Equation (2) to obtain the following dimensionless momentum equation,

$$2p_s=\frac{1}{r}\frac{d}{dr}(r\,\tau),\quad k\le r\le 1. \tag{13}$$

The dimensionless Herschel-Bulkley constitutive equation is also obtained by substituting the non-dimensional variables into Equation (5) as follows:

$$\left(\frac{\partial w}{\partial r}\right)=-\left(|\tau|-\tau_y\right)^n. \tag{14}$$

On the other hand, Equation (13) is integrated with respect to r to obtain

$$\tau=p_s r+\frac{c_1}{r}, \tag{15}$$

where c_1 is the constant of integration. Applying the boundary condition in Equation (3) into Equation (15), the following equation of

$$\tau_y=-p_s\lambda_1-\frac{c_1}{\lambda_1}, \tag{16}$$

is obtained from $r=\lambda_1$ and

$$\tau_y=p_s\lambda_2+\frac{c_1}{\lambda_2}, \tag{17}$$

is obtained from $r=\lambda_2$. Both Equations (16) and (17) are equated with each other to obtain the constant c_1 which is

$$c_1=-p_s\lambda^2, \tag{18}$$

where $\lambda^2=\lambda_1\lambda_2$. Substituting the constant c_1 into Equation (15), the following equation of shear stress is obtained

$$\tau=\frac{p_s}{r}\left(r^2-\lambda^2\right). \tag{19}$$

The dimensionless constitutive equation in Equation (14) is expanded using the binomial series expansion with the higher power term starting from $\left(\bar{\tau}_y/\bar{\tau}\right)^2$ are neglected to obtain

$$\left(\frac{\partial w}{\partial r}\right) = -\left(\tau^n - m\tau^{n-1}\tau_y\right). \tag{20}$$

The dimensionless shear stress in Equation (19) is then substituted into the constitutive equation of Herschel-Bulkley in Equation (20) to solve for the flow velocities. The bottom outer flow region, plug flow region and top outer flow region are expressed, respectively, as

$$\begin{aligned} w_o^{+} &= -p_s{}^n\left(\int_k^r\left(\frac{\lambda^2-r^2}{r}\right)^n dr - m\theta\int_k^r\left(\frac{\lambda^2-r^2}{r}\right)^{n-1} dr\right), \quad \text{for} \quad k \le r \le \lambda_1, \\ w_p &= \text{constant} \quad \text{for} \quad \lambda_1 \le r \le \lambda_2, \\ w_o^{++} &= -p_s{}^n\left(\int_r^{R(z)}\left(\frac{r^2-\lambda^2}{r}\right)^n dr - m\theta\int_r^{R(z)}\left(\frac{r^2-\lambda^2}{r}\right)^{n-1} dr\right), \quad \text{for} \quad \lambda_2 \le r \le R(z), \end{aligned} \tag{21}$$

where $\theta = \tau_y/p_s$. The integral terms in Equation (21) are solved numerically using the Simpson 3/8. The continuity condition of velocity distribution throughout the flow region leads to $w_o^{+}(r=\lambda_1) = w_p = w_o^{++}(r=\lambda_2)$, which is used to solve for λ_1 and λ_2 using the Regula-Falsi method.

Solution for dispersion function

Substituting the non-dimensional variables in Equation (12) into the unsteady convective-diffusion equation in Equation (8), the dimensionless unsteady convective-diffusion equation is obtained as

$$\frac{\partial C}{\partial t} + w\frac{\partial C}{\partial z} = \left(\frac{1}{r}\frac{\partial}{\partial r}\left(r\frac{\partial}{\partial r}\right) + \frac{1}{Pe^2}\frac{\partial^2}{\partial z^2}\right)C, \tag{22}$$

where $Pe = \bar{R}\bar{w}_0/\bar{D}_m$. The dimensionless form of the initial and boundary conditions of the Equations (9) , (10), and (11) are given by

$$\begin{aligned} C(r,z,0) &= 1 \quad \text{if} \quad |z| \le z_s/2, \\ C(r,z,0) &= 0 \quad \text{if} \quad |z| > z_s/2, \end{aligned} \tag{23}$$

$$C(r,\infty,t) = 0, \tag{24}$$

$$\frac{\partial C}{\partial r}(k,z,t) = \frac{\partial C}{\partial r}(R(z),z,t) = 0. \tag{25}$$

The convection of solute is considered to be moving across the plane with the average fluid velocity w_m. Using Equation (21), the expression for mean velocity w_m is given by

$$w_m = \frac{\int_0^{2\pi}\int_k^{R(z)} wr\ drd\psi}{\int_0^{2\pi}\int_k^{R(z)} r\ drd\psi} = \frac{2\pi\int_k^{R(z)} wr\ dr}{2\pi\left(\frac{R(z)^2}{2} - \frac{k^2}{2}\right)} = \frac{2}{R(z)^2 - k^2}\int_k^{R(z)} wr\ dr. \tag{26}$$

To solve for the solute concentration, a new coordinate system (r, z_1, t) is defined with a new axial coordinate z_1, where $z_1 = z - w_m t$. According to [14], the solution of Equation (22) is assumed to be in a series expansion as follows:

$$C(r,z,t) = C_m(z,t) + \sum_{j=1}^{\infty} f_j(r,t) \frac{\partial^j C_m(z,t)}{\partial z_1^j}, \tag{27}$$

where C_m is the mean solute concentration over a cross-section, f_j is the dispersion function and

$$C_m(z,t) = \frac{2}{\left(R(z)^2 - k^2\right)} \int_k^{R(z)} C(r,z,t) r \, dr. \tag{28}$$

The unsteady convective-diffusion equation given in Equation (22) is transformed into a coordinate system of (r, z_1, t) by substituting the definition of z_1. Equation (27) is then substituted into the transformed unsteady convective-diffusion equation to obtain

$$\begin{aligned} &\frac{\partial C_m}{\partial t} + (w - w_m)\frac{\partial C_m}{\partial z_1} - \frac{1}{Pe^2}\frac{\partial^2 C_m}{\partial z_1^2} + \sum_{j=1}^{\infty}\left[\left(\frac{\partial f_j}{\partial t} - L^2 f_j\right)\frac{\partial^j C_m}{\partial z_1^j}\right. \\ &\left. + (w - w_m) f_j \frac{\partial^{j+1} C_m}{\partial z_1^{j+1}} - \frac{1}{Pe^2} f_j \frac{\partial^{j+2} C_m}{\partial z_1^{j+2}} + f_j \frac{\partial^{j+1} C_m}{\partial t \partial z_1^j}\right] = 0. \end{aligned} \tag{29}$$

The distribution of C_m is assumed to be diffusive in nature from the starting point "zero". Thus, the GDM for C_m can be written as

$$\frac{\partial C_m}{\partial t} = \sum_{i=1}^{\infty} K_i(t) \frac{\partial^i C_m}{\partial z_1^i}. \tag{30}$$

The first two terms of Equation (30) explains the convective and diffusive transport of the mean concentration C_m along the z_1 axis, respectively. Therefore, the coefficients of K_1 and K_2 are the convection and diffusion coefficients for C_m. Substituting Equation (30) into Equation (29), the equation can be rearranged into

$$\begin{aligned} &\sum_{i=1}^{\infty} K_i(t)\frac{\partial^i C_m}{\partial z_1^i} + (w - w_m)\frac{\partial C_m}{\partial z_1} - \frac{1}{Pe^2}\frac{\partial^2 C_m}{\partial z_1^2} + \sum_{j=1}^{\infty}\left[\left(\frac{\partial f_j}{\partial t} - L^2 f_j\right)\frac{\partial^j C_m}{\partial z_1^j}\right. \\ &\left. + (w - w_m) f_j \frac{\partial^{j+1} C_m}{\partial z_1^{j+1}} - \frac{1}{Pe^2} f_j \frac{\partial^{j+2} C_m}{\partial z_1^{j+2}} + f_j \sum_{i=1}^{\infty} K_i(t) \frac{\partial^{i+j} C_m}{\partial z_1^{i+j}}\right] = 0. \end{aligned} \tag{31}$$

Equating the coefficients for the term $\partial^j C_m / \partial z_1^j$ for $j = 1,2,3,\ldots$, an infinite set of differential equations are obtained given by

$$\begin{aligned} &K_1(t) + (w - w_m) + \left(\frac{\partial f_1}{\partial t} - L^2 f_1\right) = 0, \\ &K_2(t) - \frac{1}{Pe^2} + (w - w_m) f_1 + f_1 K_1(t) + \left(\frac{\partial f_2}{\partial t} - L^2 f_2\right) = 0. \end{aligned} \tag{32}$$

From Equations (23), (24), (25), and (27), the initial and boundary conditions on the coefficient f_j are obtained as follows:

$$f_j(r,0) = 0 \quad \text{for} \quad j = 1,2,3,\ldots, \tag{33}$$

$$\frac{\partial f_{1s}}{\partial r}(r = k) = \frac{\partial f_{1s}}{\partial r}(r = R(z)) = 0, \quad \text{for} \quad j = 1,2,3,\ldots, \tag{34}$$

$$\frac{\partial f_{1t}}{\partial r}(k,t) = \frac{\partial f_{1t}}{\partial r}\left(R(z),t\right) = 0, \quad \text{for} \quad j = 1,2,3,..., \tag{35}$$

and from Equations (27) and (28), the following is obtained as

$$\int_{k}^{R(z)} f_j r \; dr = 0, \quad \text{for} \quad j = 1,2,..., \tag{36}$$

since C_m can satisfy the initial condition of C. K_1 and K_2 in Equation (32) are multiplied with r and integrated from the limit k to $R(z)$. Using the solvability condition in Equation (36), the following equations are obtained:

$$K_1 = -\frac{2}{R(z)^2 - k^2} \int_{k}^{R(z)} (w - w_m) r \; dr = 0, \tag{37}$$

$$K_2 = \frac{1}{Pe^2} - \frac{2}{R(z)^2 - k^2} \int_{k}^{R(z)} f_1 w r \; dr. \tag{38}$$

Substituting Equation (37) into Equation (32), the function f_1 can be solved from the obtained equation of

$$\frac{\partial f_1}{\partial t} - \frac{1}{r}\frac{\partial}{\partial r}\left(r\frac{\partial f_1}{\partial r}\right) + (w - w_m) = 0, \tag{39}$$

by writing the solution of Equation (39) in the form of

$$f_1(r,t) = f_{1s}(r) + f_{1t}(r,t). \tag{40}$$

Here, f_{1s} is the large time solution and f_{1t} is the time-dependent part of the solution. Substituting Equation (40) into Equation (39), the following set of equations are obtained:

$$\frac{1}{r}\frac{\partial}{\partial r}\left(r\frac{\partial f_1}{\partial r}\right) = (w - w_m), \tag{41}$$

$$\frac{\partial f_{1t}}{\partial t} = \frac{1}{r}\frac{\partial}{\partial r}\left(r\frac{\partial f_{1t}}{\partial r}\right). \tag{42}$$

The Equation (41) is solved numerically by integration with respect to r subject to the boundary conditions in Equation (34) using Simpson's 3/8 method in evaluating the integrals to obtain the solution of the steady function f_{1s}. For solving the function f_{1t}, separation of the variable method is used to solve the Equation (42) subject to the boundary conditions in Equation (35) to obtain

$$f_{1t} = \sum_{m=1}^{\infty} A_m B_0(\alpha_m r) e^{-\alpha_m^2 t}, \tag{43}$$

where $B_0(\alpha_m r) = J_1(\alpha_m k)Y_0(\alpha_m r) - Y_1(\alpha_m k)J_0(\alpha_m r)$ and

$$A_m = -\frac{\int_k^{R(z)} f_{1s} B_0 r \, dr}{\int_k^{R(z)} B_0^2 r \, dr}. \tag{44}$$

The factor α_m is the root of the equation $Y_1(\alpha_m R(z))J_1(\alpha_m k) - Y_1(\alpha_m k)J_1(\alpha_m R(z)) = 0$, where J_0, J_1 and Y_0, Y_1 are the Bessel functions of the first and second kind, respectively, with zero and first-order, respectively.

Results and Discussion

The main objective of this study is to analyze the effects of the catheter radius and stenosis size on the flow velocity and dispersion function of the Herschel-Bulkley flow through a catheterized artery with the presence of stenosis. Hence, other parameters such as the power-law index n, steady pressure gradient p_s and yield stress θ is given a constant value throughout the plotting data for the purpose of discussion on the effects of catheter radius and stenosis size except for the validation of the solution. As for the stenosis size, only the stenosis height δ is varied while the other variables affecting the stenosis size are given constant values of $l_0 = 3$, $d = 2$ and $z = 4$. The catheter radius of $0 < k < 1$ and stenosis height of $0 \leq \delta \leq 1$ are chosen to be analyzed. According to Nagarani and Sebastian [17], the catheter range of $0.1 \leq k \leq 0.3$ is the typical range in the cardiovascular system. Therefore, the effect of catheter radius is mainly analyzed at $k = 0.1, 0.2, 0.3$. Meanwhile, the stenosis height is mainly analyzed at $\delta = 0, 0.1, 0.2, 0.3$. According to Sankar and Hemalatha [7], the common values of the power-law index for blood flow usually lies between 0.9 and 1.1 and the typical value of $n = 0.95$ for $n < 1$ and $n = 1.05$ for $n > 1$ were used in their study. Nevertheless, since the main objective of this study is to analyze the effect of catheter radius and stenosis height, only one typical value of the power-law index is chosen for this present study which is $n = 0.95$. As for the yield stress, Dash et al. [20] stated that the range of $0 \leq \theta \leq 0.1$ is a suitable value for all vessels with an inserted catheter. Although their study used the yield stress values ranging from 0 to 0.3, this present study has chosen to use $\theta = 0.1$ as it is within the stated suitable range for all catheterized vessels. For the steady pressure gradient, the value of $p_s = 1$ is used in plotting the solution. The values of λ_1 and λ_2 used are obtained by solving the continuity condition of $w_o^+(r = \lambda_1) = w_o^{++}(r = \lambda_2)$ using the Regula-Falsi method, and the values are unique depending on the value of other parameters.

Validation of Solution

To validate the present solution of velocity with catheter and stenosis, the flow velocity is compared with the existing solution of Herschel-Bulkley flow velocity through a catheterized artery from [18]. The stenosis height from the present solution is set to $\delta = 0$ to nullify the effect of stenosis on the flow velocity. However, other parameters are set similar to the existing solution in which $k = 0.5$, $\theta = 0.1$, $p_s = 1$ and $n = 0.95$. Table 1 shows that the present solution is in good agreement with the existing solution as both data values are similar to each other at a chosen radius value. This indicates that the present solution is valid.

Table 1. Velocity solution comparison of the present study when $\delta = 0$ with an existing study of [18] at $k = 0.5$, $\theta = 0.1$, $p_s = 1$ and $n = 0.95$.

Radius, r	Present solution with $\delta = 0$	Existing solution with no presence of stenosis [18]
0.5	0	0
0.6	0.03477	0.03477
0.7	0.04387	0.04387
0.8	0.04353	0.04353
0.9	0.03034	0.03034
1.0	0	0

Velocity Distribution of Steady Blood Flow

The effect of catheter radius and stenosis height on the velocity of Herschel-Bulkley flow through a catheterized artery with the presence of stenosis are analyzed. Figure 2 illustrates the steady velocity through the artery at (a) $\delta = 0.1$ and $k = 0.1, 0.2, 0.3$ as well as (b) $k = 0.1$ and $\delta = 0, 0.1, 0.2, 0.3$. From Figure 2 (a), it can be observed that as the catheter radius increases, the flow velocity decreases. This is also true for when the stenosis height increases, the flow velocity decreases, as shown in Figure 2 (b). Increasing either the catheter radius when stenosis is present or stenosis height when the catheter is present decreases the radius of the flow region inside the artery. This leads to a smaller space for the red blood cells and other cell materials to flow through the artery, hence the decrease in flow velocity.

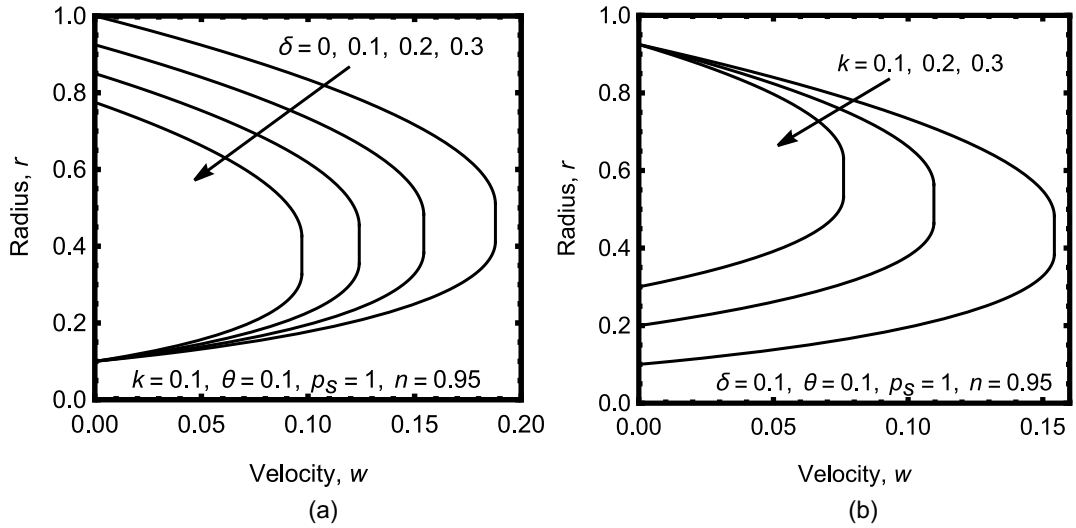

Figure 2. Variation of Herschel-Bulkley flow velocity with $\theta = 0.1$, $p_s = 1$, $n = 0.95$, $l_0 = 3$, $d = 2$ and $z = 4$ at (a) $k = 0.1$ while $\delta = 0, 0.1, 0.2, 0.3$ and (b) $\delta = 0.1$ while $k = 0.1, 0.2, 0.3$.

The flow velocity when both catheter radius and stenosis height increase simultaneously is also analyzed in Figure 3. The flow velocity significantly reduces when both catheter radius and stenosis height increase by an interval of 0.1. This is due to the higher decrease in the flow region inside the artery that leads to a significant decrease in flow velocity. Even though the increase in both catheter radius and stenosis height between intervals are similar, the decrease in velocity is different.

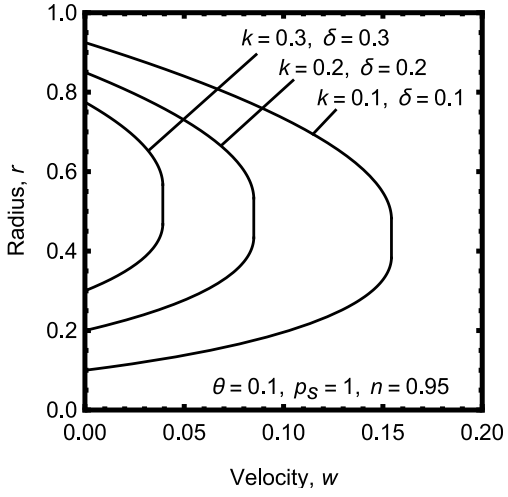

Figure 3. Variation of Herschel-Bulkley flow velocity with $\theta = 0.1$, $p_s = 1$, $n = 0.95$, $l_0 = 3$, $d = 2$ and $z = 4$ at $k = 0.1$ with $\delta = 0.1$, $k = 0.2$ with $\delta = 0.2$ and $k = 0.3$ with $\delta = 0.3$.

The blood flow behavior at the plug flow region is analyzed in Figures 4 (a) and (b). Figure 4 (a) shows the behavior of blood flow as the catheter radius increases with $\theta = 0.1$ and $\delta = 0.1$. The velocity decreases as the catheter radius increases. This is due to the decrease in the flow region in the artery as the catheter takes up more space. Since there is a presence of stenosis $\delta = 0.1$ and yield stress $\theta = 0.1$, the highest catheter radius that the velocity solution can evaluate is until $k = 0.8$. Meanwhile, in Figure 4 (b), the behavior of blood flow at the plug flow region as the stenosis height increases with $\theta = 0.1$ and $k = 0.1$ is analyzed. Similarly, the velocity at the plug flow region also decreases as the stenosis height increases due to the decrease in the flow region within the artery.

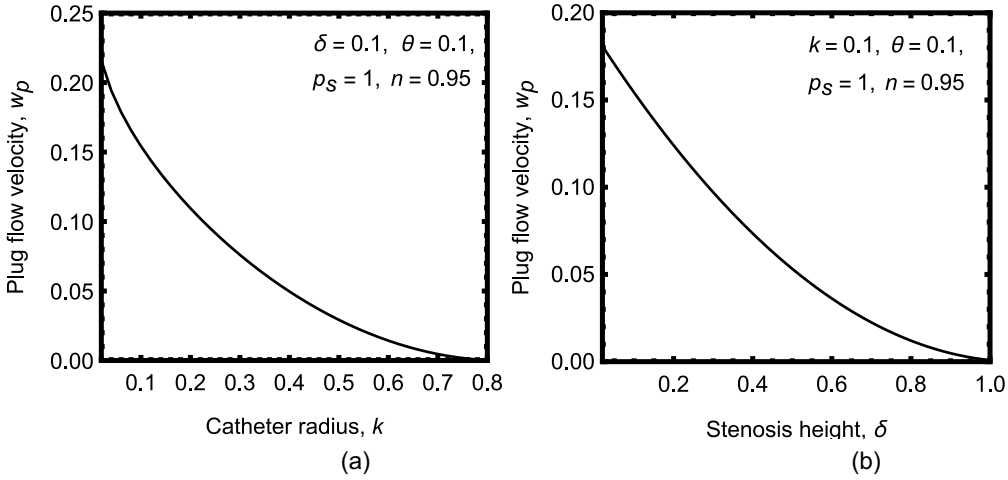

Figure 4. Variation of Herschel-Bulkley flow velocity at plug flow region with $\theta = 0.1$, $p_s = 1$, $n = 0.95$, $l_0 = 3$, $d = 2$ and $z = 4$ at (a) $\delta = 0.1$ while k is varied and (b) $k = 0.1$ while δ is varied.

Steady Dispersion Function of Solute

The dispersion function of the solute analyses the deviation of the local concentration from the mean concentration. This present study utilized the generalized dispersion model (GDM) in analyzing the dispersion function of the unsteady solute dispersion of Herschel-Bulkley fluid flowing through a catheterized artery with the presence of stenosis. The effect of catheter radius and stenosis height are observed by manipulating the value of those variables. Figure 5 shows the variation of the steady dispersion function f_{1s} with $\delta = 0.2$, $\theta = 0.1$, $p_s = 1$, $n = 0.95$, $l_0 = 3$, $d = 2$ and $z = 4$ with varying catheter radius. The catheter radius k is varied in the range of $0.1 \leq k \leq 0.3$ to analyze the influence on the steady dispersion function when there is a presence of stenosis of height $\delta = 0.2$. The graphical plot in Figure 5 exhibits a higher steady dispersion function at the wall of the artery compared to the centre of the artery. At the centre of the artery, the steady dispersion function decreases as the radius approaches the plug flow region. Meanwhile, from the plug flow region to the wall of the artery, the steady dispersion function increases. Nevertheless, as the catheter radius increases, the steady dispersion function increases. This is due to the narrowing of the artery, which leads to a decrease in flow velocity. Slower velocity causes the solute dispersion in the particular region to further disperse in that area due to the slower movement along the axial direction of the artery.

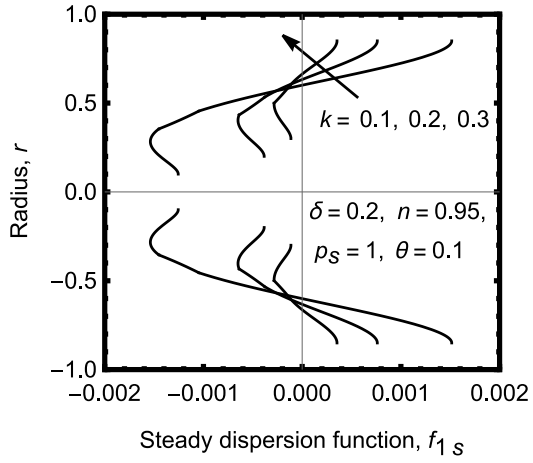

Figure 5. Variation of steady dispersion function with $\delta = 0.2$, $\theta = 0.1$, $p_s = 1$, $n = 0.95$, $l_0 = 3$, $d = 2$ and $z = 4$ with varying catheter radius of $k = 0.1, 0.2, 0.3$.

In Figure 6, the effect of stenosis height on the steady dispersion function f_{1s} with $k = 0.2$, $\theta = 0.1$, $p_s = 1$, $n = 0.95$, $l_0 = 3$, $d = 2$ and $z = 4$ with varying stenosis height are investigated. The stenosis size depends on the value of the stenosis height δ, which is varied in the range of $0 \leq \delta \leq 0.3$ to analyze the influence on the steady dispersion function when there is a presence of the catheter. It can be observed that the pattern behavior of steady dispersion function is almost similar when the catheter radius is varied, as in Figure 6. The steady dispersion function is higher at the wall of the artery compared to the centre of the artery. Not to mention a decrease in steady dispersion function from the centre of the artery towards the plug flow region and vice versa from the plug flow region to the wall of the artery. However, the increase in stenosis height increases the steady dispersion function. The reasoning is similar to when the catheter radius increases. An increase in stenosis height leads to a decrease in the flow region. Consequently, the flow velocity decreases and solutes in the particular region are able to disperse more effectively.

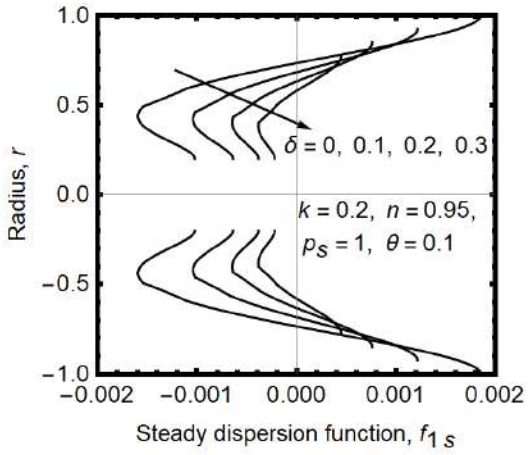

Figure 6. Variation of steady dispersion function with $k = 0.2$, $\theta = 0.1$, $p_s = 1$, $n = 0.95$, $l_0 = 3$, $d = 2$ and $z = 4$ with varying stenosis height of $\delta = 0, 0.1, 0.2, 0.3$.

Unsteady Dispersion Function of Solute

For the unsteady dispersion function f_{1t}, the dispersion process is affected by the time parameter. The effect of catheter radius and stenosis height on the unsteady dispersion function is investigated when the time variable is varied. The variation of unsteady dispersion function with $\delta = 0.2$, $\theta = 0.1$, $p_s =$

1, $n = 0.95$, $l_0 = 3$, $d = 2$, $z = 4$ and $t = 0.1$ with varying catheter radius of $k = 0.1, 0.2, 0.3$ are shown in Figure 7. It can be noted that the unsteady dispersion function is higher at the centre of the artery compared to the wall of the artery. As the catheter radius increases, the unsteady dispersion function at the wall of the artery increases more when $k = 0.3$ compared with $k = 0.1$. This is due to the smaller flow region and decrease in flow velocity that leads to a more effective unsteady dispersion.

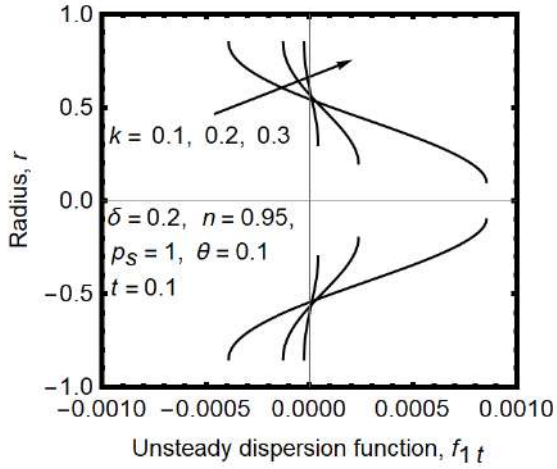

Figure 7. Variation of unsteady dispersion function with $\delta = 0.2$, $\theta = 0.1$, $p_s = 1$, $n = 0.95$, $l_0 = 3$, $d = 2$, $z = 4$ and $t = 0.1$ with varying catheter radius of $k = 0.1, 0.2, 0.3$.

Similarly, the unsteady dispersion function also increases when the stenosis height increases, as depicted in Figure 8, where the stenosis height is varied. This is due to the reduction of flow region and flow velocity when the stenosis height increases. This increases the effectiveness of the unsteady dispersion. It can also be noted that the increment of unsteady dispersion function from the wall of the artery to the centre of the artery at $\delta = 0$ is more rapid compared to the other stenosis height. Again, this is due to the high velocity as the flow region is bigger.

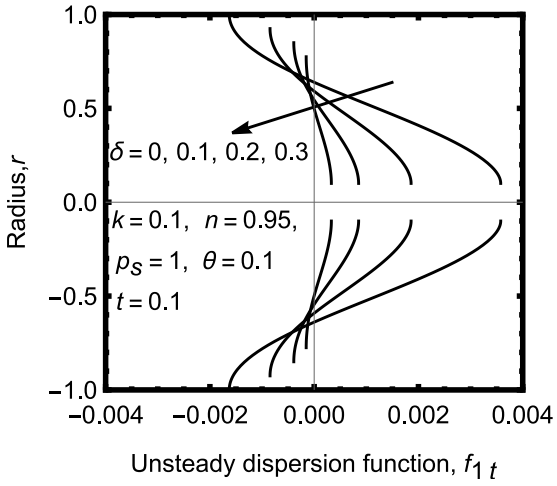

Figure 8. Variation of unsteady dispersion function at $k = 0.1$, $\theta = 0.1$, $p_s = 1$, $n = 0.95$, $l_0 = 3$, $d = 2$, $z = 4$ and $t = 0.1$ with varying stenosis height of $\delta = 0, 0.1, 0.2, 0.3$.

In Figure 9, the unsteady dispersion function at the artery radius of $r = 0.5$ with both catheter and stenosis present are analyzed when the time t is varied between $0.1 \leq t \leq 0.3$. It can be observed that the unsteady dispersion of function when $k = 0.1$, $\theta = 0.1$, $p_s = 1$, $n = 0.95$, $l_0 = 3$, $d = 2$, and $z = 4$

decreases at the time increase from 0.1 to 0.3. It can be noted that a decrease in unsteady dispersion function from $t = 0.1$ to $t = 0.2$ is substantially higher compared to the decrease in unsteady dispersion function from $t = 0.2$ to $t = 0.3$. After some time, the unsteady dispersion function reaches a constant state.

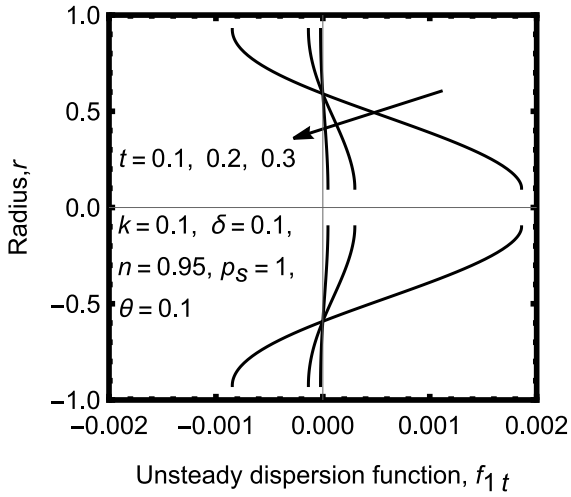

Figure 9. Variation of unsteady dispersion function at $k = 0.1$, $\delta = 0.1$, $\theta = 0.1$, $p_s = 1$, $n = 0.95$, $l_0 = 3$, $d = 2$ and $z = 4$ with varying time of $t = 0.1, 0.2, 0.3$.

Dispersion Function of Solute

The dispersion function f_1 is the combination of the steady dispersion function and unsteady dispersion function. The effect of catheter radius and stenosis height on the dispersion function is investigated. Figure 10 illustrates the dispersion function at $\delta = 0.2$, $\theta = 0.1$, $p_s = 1$, $n = 0.95$, $l_0 = 3$, $d = 2, z = 4$ and $t = 0.1$ with varied catheter radius of $k = 0.1, 0.2, 0.3$. From the figure, it can be observed that the dispersion function increases as the catheter radius increases. The dispersion function is the lowest at the centre of the artery and highest at the wall of the artery. Additionally, the highest and lowest dispersion function occurs at $k = 0.1$. This is due to the larger flow region and higher velocity. Thus, the change in dispersion function is more prominent compared to $k = 0.2$ and $k = 0.3$. Nevertheless, in the radius range of 0.5 to 0.6, the increment in dispersion function at $k = 0.1$ intersect and surpasses the increment of dispersion function at $k = 0.2$ and $k = 0.3$.

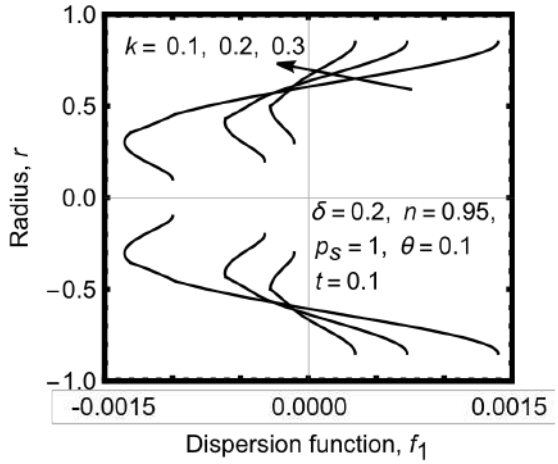

Figure 10. Variation of dispersion function at $\delta = 0.2$, $\theta = 0.1$, $p_s = 1$, $n = 0.95$, $l_0 = 3$, $d = 2$, $z = 4$ and $t = 0.1$ with varying catheter radius of $k = 0.1, 0.2, 0.3$.

Figure 11 shows the dispersion function at $k = 0.1$, $\theta = 0.1$, $p_s = 1$, $n = 0.95$, $l_0 = 3$, $d = 2$, $z = 4$ and $t = 0.1$ with varied stenosis height of $\delta = 0, 0.1, 0.2, 0.3$. As the stenosis height increases, the dispersion function increases. The behavior of the dispersion function is almost similar to when the catheter radius is varied in which the dispersion function is low at the centre of the artery and high at the wall of the artery. However, the increase of dispersion function from the centre of the artery to the wall of the artery is more uniform in approaching the arterial wall compared to the varying catheter radius in Figure 10. Here, the increase in dispersion function is more diverse after the intersection point between the range 0.5-0.6.

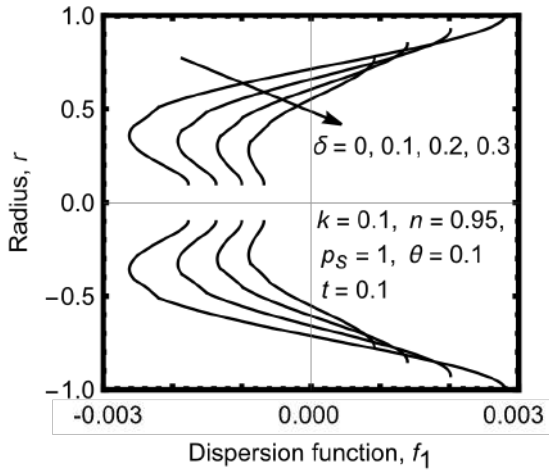

Figure 11. Variation of dispersion function at $k = 0.1$, $\theta = 0.1$, $p_s = 1$, $n = 0.95$, $l_0 = 3$, $d = 2$, $z = 4$ and $t = 0.1$ with varying stenosis height of $\delta = 0, 0.1, 0.2, 0.3$.

Application to a Catheterized Artery with Presence of Stenosis

The formation of stenosis at the wall of the artery is one of the main factors that contribute to cardiovascular disease. Besides narrowing the flow region inside the artery, stenosis could also potentially dislodge from the arterial wall and travel to the brain leading to a stroke attack. To prevent this situation, catheterization of the artery is required to perform a medical procedure to reduce the size of the stenosis. By understanding the behavior of blood flow and solute dispersion when both catheter and stenosis are present, doctors and medical practitioners can choose to control the catheter size depending on the stenosis size of a patient. This can reduce the risk of complications for the patient. Not to mention, there are various types of arteries inside the human circulatory system, and each artery has a different radius. The type of artery that doctors will perform the catheterization depends on the location of stenosis in the body. Therefore, the blood flow velocity and solute dispersion behavior in those arteries must be studied to minimize the risk of complications.

Physiological data of several artery radii from Das and Saha [21] are used to study the behavior of blood flow velocity and solute dispersion function. Aorta is the main artery that carries the blood from the heart to the rest of the body. Meanwhile, the femoral artery is the main artery that supplies blood to the lower part of the body. Note that the carotid artery is an artery located in the neck region that supplies blood to the head and brain. Table 2 shows that the biggest artery is the aorta compared to the femoral and carotid arteries. The blood flow velocity and solute dispersion function are analyzed at the plug flow region of the lower plane λ_1.

It can be noted that the increase in the artery radius increases the flow velocity at $r = \lambda_1$ of the artery even when there is a presence of catheter and stenosis of $k = 0.1$ and $\delta = 0.1$, respectively. This is because a larger artery radius has a larger flow space for blood to flow smoothly. Therefore, if a medicine injected through the catheter is required to travel quickly, doctors should consider the largest artery available. However, the dispersion function decreases as the artery radius increases. Therefore, when

a medicine is required to disperse effectively at a certain region, a smaller artery is advised to be used. For example, using a drug-eluting stent coated with medicine is placed at the site of stenosis. Drugs such as sirolimus, its derivatives and paclitaxel have been used to coat the drug-eluting stent to prevent restenosis and stent thrombosis [22]. Therefore, the placement of such a stent at a smaller artery with high dispersion function is beneficial for patients.

Table 2. Flow velocity and dispersion function of varying artery radius at the centre of the artery with $k = 0.1$, $\delta = 0.1$, $\theta = 0.1$, $p_s = 1$, $n = 0.95$, $l_0 = 3$, $d = 2$ and $z = 4$.

Artery	Artery radius	Radius at plug flow, λ_1	Velocity, W	Dispersion function, f_1
Aorta	1	0.5	0.00399229	-0.001866
Femoral	0.5	0.25	0.000376356	-0.000043
Carotid	0.4	0.2	0.000371868	-0.000008

Conclusions

In conclusion, the effect of catheter radius and stenosis size on the behavior of steady flow velocity and unsteady solute dispersion through a catheterized artery with the presence of stenosis can be investigated by manipulating the catheter radius and stenosis height. Other variables such as n, p_s, θ, z, d, l_0 are given a constant value. It can be noted that an increase in either the catheter radius or stenosis height decreases the blood flow velocity. This is due to the decrease in the flow region that causes red blood cells to flow in a much smaller space leading to an accumulation of red blood cells. Hence, the flow velocity decreases. In the case of both catheter radius and stenosis height increase simultaneously, the decrease in flow velocity is significantly higher compared to when only either catheter radius or stenosis height increases. This is because the decrease in the flow region is more substantial when both catheter radius and stenosis height increase compared to when only either catheter radius or stenosis height increases. As for the steady dispersion function, an increase in either the catheter radius or stenosis height increases the steady dispersion function. The smaller flow region caused by the increase in either catheter radius or stenosis height leads to a slower flow velocity and causes the solute to disperse more effectively at a particular region. For the unsteady dispersion function, the effect of catheter radius and stenosis height on the unsteady dispersion function is similar to the behavior of the steady dispersion function. Increase in catheter radius and stenosis height increases the unsteady dispersion function. The time parameter in the unsteady dispersion function also influences the unsteady dispersion function. As time increases, the unsteady dispersion function decreases. The dispersion function f_1 is the summation of the steady and unsteady dispersion function. Therefore, the dispersion function exhibits a similar behavior of increment when the catheter radius and stenosis height increase. The result obtained from the mathematical analysis concluded that the catheter radius and stenosis height highly influence the flow velocity and dispersion function. Both variables should be considered when introducing a catheter into an artery that has a presence of stenosis as it changes the behavior of blood flow and solute dispersion. Therefore, this present study contributes a significant advancement in the mathematical modelling field of steady flow and unsteady dispersion through a catheterized artery with the presence of stenosis.

Conflicts of interest

The authors declare that there is no conflict of interest regarding the publication of this paper.

Acknowledgments

This research was supported by the Ministry of Education (MOE) through Fundamental Research Grant Scheme (FRGS/1/2020/STG06/UTM/02/15) and also carried up under the research grant GUP Tier 2 (Vote number Q.J130000.2654.17J12).

References

[1] Ali, N., Zaman, A., Sajid, M., Nieto, J. J., & Torres, A. (2015). Unsteady non-Newtonian blood flow through a tapered overlapping stenosed catheterized vessel. *Mathematical biosciences, 269*, 94-103.

[2] Ullah, I., Shafie, S., & Khan, I. (2017). MHD free convection flow of Casson fluid over a permeable nonlinearly stretching sheet with chemical reaction. *Malaysian Journal of Fundamental and Applied Sciences*, *13*(3), 263-270.

[3] Srivastava, V. P., & Srivastava, R. (2009). Particulate suspension blood flow through a narrow catheterized artery. *Computers & Mathematics with Applications*, *58*(2), 227-238.

[4] Sriyab, S. (2014). Mathematical analysis of non-Newtonian blood flow in stenosis narrow arteries. *Computational and mathematical methods in medicine*, *2014*.

[5] Nagarani, P., Sarojamma, G., & Jayaraman, G. (2006). Exact analysis of unsteady convective diffusion in Casson fluid flow in an annulus–Application to catheterized artery. *Acta mechanica*, *187*(1), 189-202.

[6] Sarojamma, G., Vishali, B., & Ramana, B. (2012). Flow of blood through a stenosed catheterized artery under the influence of a body acceleration modelling blood as a Casson fluid. *International Journal of Applied Mathematics and Mechanics*, *8*(11), 1-17.

[7] Sankar, D. S., & Hemalatha, K. (2006). Pulsatile flow of Herschel-Bulkley fluid through stenosed arteries–A mathematical model. *International Journal of Non-Linear Mechanics*, *41*(8), 979-990.

[8] Chaturani, P., and Ponnalagar Samy, R. (1985). A study of non-Newtonian aspects of blood flow through stenosed arteries and its applications in arterial diseases. *Biorheology*, *22*, 521-531.

[9] Sankar, D. S., & Lee, U. (2008). Two-fluid Herschel-Bulkley model for blood flow in catheterized arteries. *Journal of Mechanical Science and Technology*, *22*(5), 1008.

[10] Sankar, D. S., & Hemalatha, K. (2007). Pulsatile flow of Herschel-Bulkley fluid through catheterized arteries–A mathematical model. *Applied Mathematical Modelling*, *31*(8), 1497-1517.

[11] Abidin, S. N. A. M. Z., Jaafar, N. A., & Ismail, Z. (2021). Herschel-Bulkley model of blood flow through a stenosed artery with the effect of chemical reaction on solute dispersion. *Malaysian Journal of Fundamental and Applied Sciences, 17*(4), 457-474.

[12] Taylor, G. I. (1953). Dispersion of soluble matter in solvent flowing slowly through a tube. Proceedings of the Royal Society of London. Series A. *Mathematical and Physical Sciences, 219*(1137), 186-203.

[13] Aris, R. (1956). On the dispersion of a solute in a fluid flowing through a tube. *Proceedings of the Royal Society of London. Series A. Mathematical and Physical Sciences, 235*(1200), 67-77.

[14] Gill, W. N., & Sankarasubramanian, R. (1970). Exact analysis of unsteady convective diffusion. *Proceedings of the Royal Society of London. A. Mathematical and Physical Sciences, 316*(1526), 341-350.

[15] Nagarani, P., Sarojamma, G., & Jayaraman, G. (2008). On the dispersion of a solute in a Casson fluid flow in an annulus with boundary absorption. In *American Conference on Applied Mathematics (MATH'08)*, 265-273.

[16] Ramana, B., & Sarojamma, G. (2013). Exact analysis of unsteady convective diffusion in a Herschel-Bulkley fluid in an annular pipe. *International Journal of Mathematics and Computer Applications Research, 3*(1), 15-26.

[17] Nagarani, P., & Sebastian, B. T. (2017). Effect of flow unsteadiness on dispersion in non-Newtonian fluid in an annulus. *Journal of applied mathematics & informatics, 35*(3-4), 241-260.

[18] Sankar, D. S., & Hemalatha, K. (2007). A non-Newtonian fluid flow model for blood flow through a catheterized artery–Steady flow. *Applied mathematical modelling*, *31*(9), 1847-1864.

[19] Jaafar, N. A., Zainul Abidin, S. N. M., Ismail, Z., & Mohamad, A. Q. (2021). Mathematical analysis of unsteady solute dispersion with chemical reaction through a stenosed artery. *Journal of Advanced Research in Fluid Mechanics and Thermal Sciences, 86*(2), 56-73.

[20] Dash, R. K., Jayaraman, G., & Mehta, K. N. (1996). Estimation of increased flow resistance in a narrow catheterized artery–A theoretical model. *Journal of Biomechanics*, *29*(7), 917-930.

[21] Das, K., & Saha, G. C. (2009). Arterial MHD pulsatile flow of blood under periodic body acceleration. *Bulletin of Society of Mathematicians Banja Luka*, *16*, 21-42.

[22] Lukman, S. K., Al-Ashwal, R. H., Khudzari, A. Z. M., & Saidin, S. (2019). Emerging of cardiovascular metal stent: A review on drug-eluting stent towards the utilisation of herbal coating. *Malaysian Journal of Fundamental and Applied Sciences, 15*, 225-231.